

PCCP

Accepted Manuscript



This is an *Accepted Manuscript*, which has been through the Royal Society of Chemistry peer review process and has been accepted for publication.

Accepted Manuscripts are published online shortly after acceptance, before technical editing, formatting and proof reading. Using this free service, authors can make their results available to the community, in citable form, before we publish the edited article. We will replace this *Accepted Manuscript* with the edited and formatted *Advance Article* as soon as it is available.

You can find more information about *Accepted Manuscripts* in the [Information for Authors](#).

Please note that technical editing may introduce minor changes to the text and/or graphics, which may alter content. The journal's standard [Terms & Conditions](#) and the [Ethical guidelines](#) still apply. In no event shall the Royal Society of Chemistry be held responsible for any errors or omissions in this *Accepted Manuscript* or any consequences arising from the use of any information it contains.

Magnetically Recoverable Ni/C Catalysts with Hierarchical Structure and High-Stability for Selective Hydrogenation of Nitroarenes

Cite this: DOI:
10.1039/x0xx00000x

Peng Zhang¹, Chang Yu¹, Xiaoming Fan¹, Xiuna Wang¹, Zheng Ling¹, Zonghua Wang² and Jieshan Qiu^{1*}

Received 00th January 2012,
Accepted 00th January 2012

DOI: 10.1039/x0xx00000x

www.rsc.org/

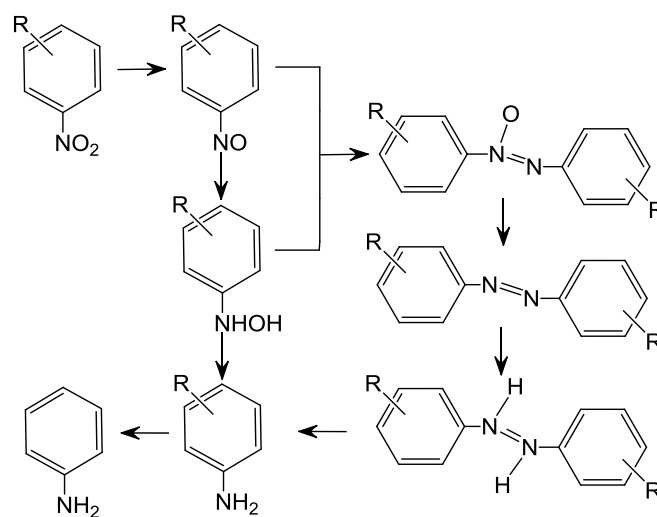
Here we report that magnetic Ni/C catalysts with hierarchical structure can be fabricated from a mixture of nickel acetate, polyethylene glycol-200 and furfural by one-step hydrothermal method, followed by calcination. It has been found that the calcination temperature is the key factor affecting the structure, morphology and the catalytic performance of the Ni/C catalysts. Of the as-made catalysts, the Ni/C sample calcined at 300 °C features small-size metallic Ni particles in high dispersion in the carbon matrix and unique hierarchical structure, and has the highest conversion of *o*-chloronitrobenzene with high selectivity to *o*-chloroanilines. The concerned Ni/C catalysts are magnetic due to the presence of metallic Ni particles, which makes it easily to be recovered after the reaction by an external magnetic field. The recovered Ni/C catalysts can be recycled for at least ten times without obvious loss both in the Ni loading and the catalytic performance. This kind of catalyst is also active for the selective hydrogenation of other nitroarenes to the corresponding anilines.

Introduction

Anilines are important intermediates for the production of organic chemical products such as dyes, drugs, herbicides and pesticides, usually made by hydrogenating nitroarenes. The pathways and mechanism involved in the reaction are very complicated, as shown in Scheme 1, in which many undesired by-products may be formed.¹⁻³ To tackle this problem, catalysts with high activity and selectivity are highly required. Up to now, many noble metal catalysts such as Pt,⁴⁻⁷ Pd,⁸ Au,⁹⁻¹¹ Ag,¹² and Ru¹³ have been developed, which show a high conversion of substrates, and can effectively suppress the formation of by-products. However, the high cost of the noble metals has limited their practical use. It has been found that the supported metallic Ni catalysts¹⁴⁻¹⁸ are one of the ideal candidates for the selective hydrogenation of nitroarenes due to their high catalytic activity and low cost. Moreover, the unique magnetic property of metallic Ni particles makes it attractive because the catalysts can be recovered after the reaction by an external magnetic field, and this would greatly reduce the cost in the industrial practice.¹⁹

Carbon materials are excellent catalyst supports for the selective hydrogenation of nitroarenes, owing to their intrinsic properties such as high surface area, unique electronic property and chemical inertness as well as thermal stability and high mechanical strength.²⁰⁻²⁵ However, for the carbon-based catalysts available now, the production procedure is time-consuming and complex.^{21,22} As such, it is highly desirable to develop a simple, efficient and sustainable route to synthesize

active Ni/C catalysts for the selective hydrogenation of nitroarenes, and this remains a challenge.



Scheme 1. The possible reaction pathways involved in hydrogenation of nitroarenes.

Of various carbon materials, biomass-based hydrothermal carbon (HTC) materials have received an increasing interest due to their good sustainability, tunable surface chemistry and porous structure.^{26,27} More importantly, they can be easily

incorporated with metals or metallic oxides to make functional composites that have been successfully used in various fields such as energy,²⁸⁻³⁰ catalysis,^{31,32} and environment protection.³³ Here, we report a facile one-step hydrothermal method to prepare sheet-like Ni/C catalyst precursors with furfural, a biomass derivative, as the carbon source. After heating the precursor at different temperatures, a series of Ni/C catalysts with unique hierarchical structure were prepared, which show high catalytic activities and selectivities for the hydrogenation of *o*-chloronitrobenzene (*o*-CNB) to *o*-chloroanilines (*o*-CAN). Compared with other samples, the catalyst made at 300 °C shows the best catalytic performance and a good stability, evidenced by a high conversion of *o*-CNB and selectivity to *o*-CAN even after 10 cycles. The Ni/C catalyst is also active for the selective hydrogenation of other nitroarenes to the corresponding anilines.

Experimental

Preparation of the catalysts

All of the reagents involved in present study were of analytical grade, and used without further purification. The low-temperature hydrothermal method was used to make the precursor of Ni/C catalysts. For a typical run, 0.6 g of nickel acetate, 32 mL of polyethylene glycol-200 (PEG-200) and 1 mL of furfural were added into 32 mL of deionized water under magnetic stirring at room temperature, yielding a clear solution in which all gradients were completely dissolved. The clear solution was transferred into a 100 mL Teflon-lined autoclave, sealed, and maintained at 180 °C for 12 h. When the reaction finished, the autoclave was naturally cooled back to room temperature, yielding powder-like products that were collected by filtering, and washed with deionized water and absolute ethanol for three times. After dried at 80 °C for 3 h under vacuum, the hydrothermal product finally was obtained and used as the precursor of Ni/C catalysts, which was named as Ni/C-p. The as-obtained Ni/C-p was put in a tube furnace, ramped at 3 °C/min in flowing H₂ to different temperatures, and kept at the final temperature for 3 h, yielding the Ni/C catalysts named as Ni/C-T, where T refers to the calcination temperature.

Characterization of the catalysts

The morphology and structure of the as-made catalysts were examined by scanning electron microscopy (SEM, Quanta 450), transmission electron microscopy (TEM, JEM-2000EX), high resolution transmission electron microscopy (HRTEM, Philips Tecnai G220), and energy-dispersive X-ray spectrometry (EDX, Oxford X-Max). Fourier transform infrared (FTIR) spectra were measured by a Thermo Nicolet 6700 Flex with KBr as the reference. The X-ray diffraction patterns (XRD) were recorded on a Rigaku D/Max-2400X apparatus with Cu K α irradiation, operated at 40 kV and 100 mA. The average sizes of Ni particles in catalysts were calculated using the Scherrer equation. N₂ adsorption-desorption isotherms of the Ni/C catalysts were measured by Micromeritics ASAP 2020 at -196 °C, and their pore size distributions were calculated by DFT model. Before the measurement, the samples were degassed at 200 °C for 5 h under vacuum.

Hydrogenation of nitroarenes

The selective hydrogenation of nitroarenes was carried out in a 100 mL Parr 4843 autoclave. Typically, the autoclave was loaded with 0.05 g of catalyst, 0.50 g of substrates and 50 mL of ethanol, then was completely sealed and flushed for three times with pure hydrogen to remove air. After introducing H₂ at an initial pressure of 2.0 MPa, the reactor was heated to 140 °C under constant stirring, and held at 140 °C for 1~2 h. After the reaction, the autoclave was cooled back to room temperature, and the reaction mixture was separated by a magnet, of which the solution was analysed by gas chromatography (GC, Techcomp 7890F, equipped with SE-54 capillary column and a flame ionization detector). For the Ni/C-300 catalyst, it was collected, washed with absolute ethanol for three times, and dried at 80 °C before reuse.

Results and Discussion

The typical SEM image of the as-made Ni/C-p is shown in Figure 1a, showing a nanosheet-shaped structure with a thickness of 40~50 nm. Further TEM examination of the Ni/C-p (Figure 1b) reveals that the nanosheets are interconnected with each other, and exist as a bundle of agglomerated sheets. The FTIR spectrum (Figure 1c) shows a sharp peak at 3600 cm⁻¹, corresponding the geminal OH groups in the brucite-like structure,^{34,35} and peaks at *ca.* 3500, 1700 and 1000~1300 cm⁻¹ that can be assigned to the stretching vibration of -OH, COO⁻ and other oxygen-containing groups.^{36,37} The FTIR analysis suggests that the surface chemistry of the Ni/C-p is similar to the HTC. The EDX results (Figure 4d) also confirm the presence of C, O, and Ni species in Ni/C-p, while the Ni species are present in the form of Ni(OH)₂, confirmed by the XRD data discussed below.

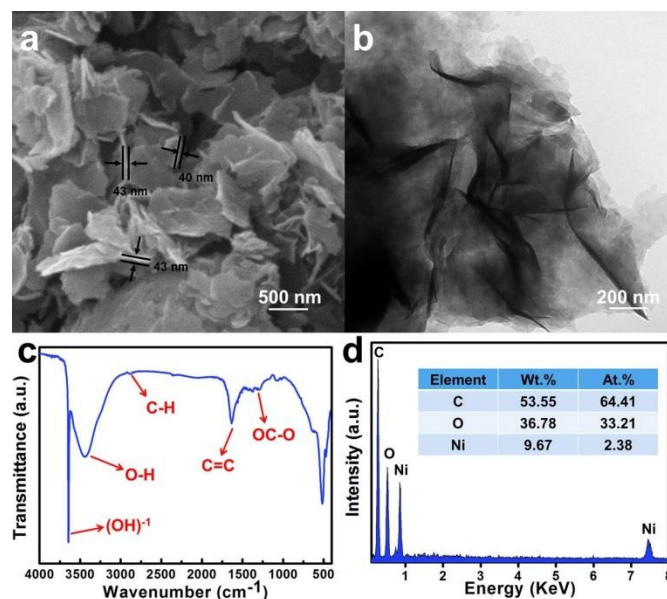


Figure 1. (a) Typical SEM image, (b) TEM image, (c) FTIR spectrum, and (d) EDX spectrum of the Ni/C-p.

The catalysts made at different calcination temperatures were analyzed by XRD, of which the results are shown in Figure 2. It can be clearly seen that the components of the catalysts vary with the

calcination temperature. For the Ni/C-p and Ni/C-200, Ni species are mainly Ni(OH)₂, and no peaks related to metallic Ni can be seen. When the calcination temperature increases to 300 °C or higher, the characteristic peaks of Ni(OH)₂ disappear, and new peaks of metallic Ni species can be observed,²² indicating that Ni(OH)₂ species in the Ni/C-p are reduced to metallic Ni particles at 300 °C or above in H₂. Obviously, except for the Ni/C-p and Ni/C-200, all of the catalysts obtained in the present study contain metallic Ni species.

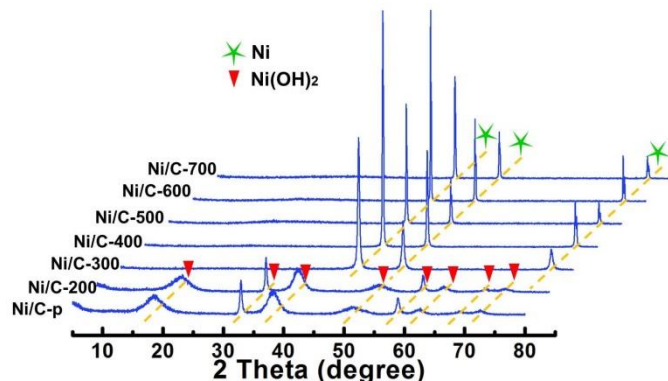


Figure 2. XRD patterns of the Ni/C-p and Ni/C catalysts made at different calcination temperatures.

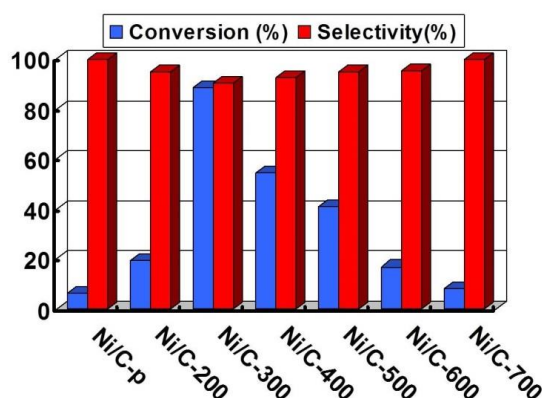


Figure 3. The catalytic performance of Ni/C catalysts for selective hydrogenation of *o*-CNB. Reaction conditions: 0.50 g *o*-CNB, 0.05 g catalyst, 50 mL ethanol, 140 °C, 2.0 MPa H₂, time 1 h.

The catalytic performance of different Ni/C catalysts for the selective hydrogenation of *o*-CNB to *o*-CAN was evaluated, of which the results are shown in Figure 3 and Table S1. It can be seen that all of the Ni/C catalysts used in the present work show catalytic activities to some degree, with a selectivity to *o*-CAN over 90%. In particular, the Ni/C-300 shows a much better activity than other catalysts under the same conditions (140 °C, 2 MPa H₂, 1 h) in terms of both *o*-CNB conversion of 88.4% and *o*-CAN selectivity of 90.4%, and reaches nearly 100% in conversion of *o*-CNB in 2 h. Compared with the Ni/C-p and Ni/C-200, the enhanced catalytic performance of Ni/C-300 can be attributed to the formation of metallic Ni species, evidenced by XRD results shown in Figure 2. For the Ni/C catalysts obtained at temperatures over 300 °C, the catalytic activity drops greatly in terms of the *o*-CNB conversion as the calcination temperature increases. This is mainly due to the aggregation of the Ni particles, the decrease of the surface area and the destruction of porous structure of Ni/C catalysts, which will be further discussed below.

Figure 4 is the typical SEM and TEM images of the Ni/C-300, showing that the nanosheets in the Ni/C-p are transformed into irregular spherical assemblies (Figure 4a) after calcination at 300 °C, mainly due to the shrinkage of hydrothermal carbon nanosheets^{37,38} and the aggregation of metallic Ni particles.³⁹ The magnified SEM image (Figure 4b) shows that the Ni/C-300 has a unique hierarchical structure made of sheet-like subunits. Figure 4c is the TEM image of Ni/C-300, in which many pores made of disorderly assembled sheet-like subunits can be seen, which would provide channels for the transportation of reactants and products. Higher resolution TEM image (Figure 4d) shows that metallic Ni particles are abundant, evenly embedded in the nanosheet-like carbon matrix, and have a narrow size distribution of 5~15 nm (Figure 4f) with an average size of *ca.* 9 nm. Besides, the HRTEM image of the Ni/C-300 (Figure 4e) reveals that the Ni particle has the perfect single-crystal structure. The interplanar distance can be measured to be about 2.04 Å, assigning to the lattice plane of Ni (111). It is because of the relatively uniform and small-sized Ni particles that the Ni/C-300 catalyst shows superior catalytic performance for the selective hydrogenation of *o*-CNB to *o*-CAN.

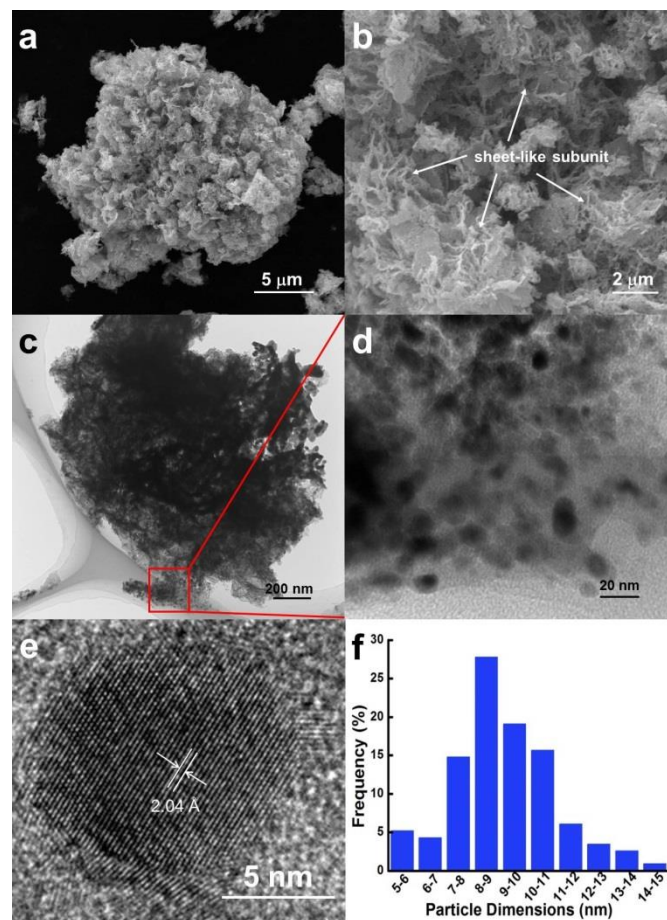


Figure 4. (a) SEM image, (b) high-magnification SEM image, (c) typical TEM image, and (d) magnified TEM image of the Ni/C-300, (e) HRTEM image and (f) size distribution of Ni particles in the Ni/C-300.

Figure S1-S4 are the SEM and TEM images of the Ni/C catalysts calcined at temperatures over 300 °C, showing

obvious difference from the Ni/C-300. For the Ni/C-400 catalyst, the sheet-like subunits disappear, instead, the irregular particle subunits are formed (Figure S1a), and meanwhile, the size of metallic Ni particles increases dramatically (Figure S1b and S1c). As the calcination temperature increases further, the subunits in irregular spherical catalyst gradually collapse (Figure S2-S3). In the case of the Ni/C-700, its hierarchical structure is completely destroyed, evidenced by its SEM (Figure S4a) and TEM images (Figure S4b) in which a compact instead of the porous structure is observed. The magnified TEM image (Figure S4c) shows that it is hard to see a monodispersed Ni particle in the carbon matrix, which may be due to the agglomeration of the metallic Ni particles in the Ni/C-700. According to the Scherrer equation, the average sizes of Ni particles in the Ni/C-400, Ni/C-500, Ni/C-600, and Ni/C-700 are 35, 46, 56, and 65 nm, respectively. Nevertheless, the crystal structure characteristics of the Ni particles remain unchanged, which are confirmed by HRTEM images of the Ni/C-400 and Ni/C-700 (Figure S1d and S4d).

In addition, the destruction of hierarchical structure in Ni/C catalysts resulted in a smaller surface area. Figure S5 is the N₂ adsorption-desorption isotherms, showing that the N₂ adsorption amount of Ni/C-300 is much higher than Ni/C-400, and their Brunauer-Emmett-Teller (BET) specific surface areas are 20.0 and 8 m²/g, respectively. This is further confirmed by the disappeared micropores and mesopores in Ni/C-400, as the pore size distributions of the Ni/C-300 and Ni/C-400 shown in Figure S6. Obviously, higher calcination temperature would result in the collapse of hierarchical structure and the agglomeration of Ni particles, thus leading to poorer catalytic performance of Ni/C catalyst for the selective hydrogenation of *o*-CNB, as shown in Figure 3.

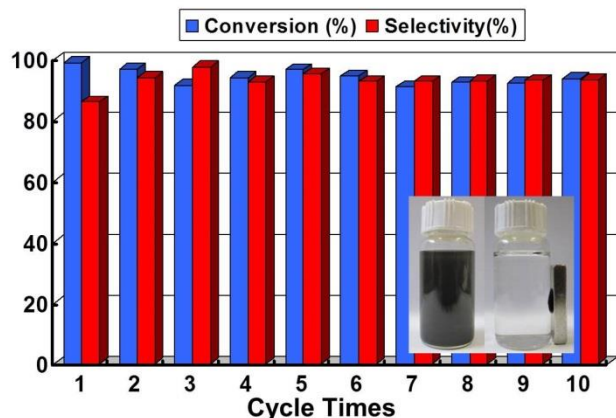


Figure 5. Cycling performance of the Ni/C-300 for selective hydrogenation of *o*-CNBN. Reaction conditions: 0.50 g *o*-CNBN, 0.05 g Ni/C-300, 50 mL ethanol, 140 °C, 2.0 MPa H₂, time 2 h. Inset shows the separation of the Ni/C-300 with a magnet after the reaction.

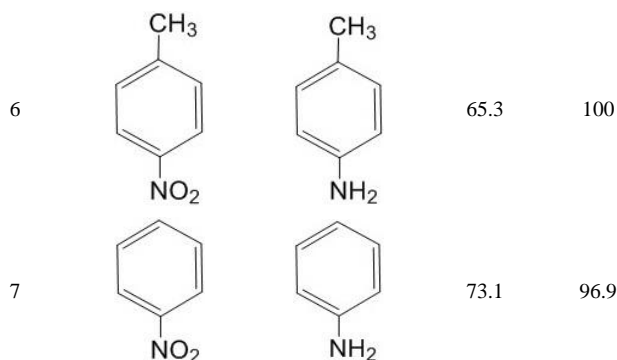
For high performance catalysts, in addition to the catalytic activity and selectivity, their stability is another important issue. The catalytic stability of the Ni/C-300 catalyst was also evaluated by the hydrogenation of *o*-CNBN to *o*-CAN in the present work, of which the results are shown in Figure 5 and Table S2. It can be seen that no obvious drop in both the *o*-CNBN conversion and the *o*-CAN selectivity is observed over the Ni/C-300 catalyst, even after ten cycles. Both the *o*-CNBN conversion and selectivity to *o*-CAN are over 90% under reaction conditions of 140 °C, 2 MPa H₂, time 2 h. Moreover, the supported metallic Ni particles that are magnetic make the

Ni/C-300 to be easily separated from the solution by an external magnetic field, as shown in inset of Figure 5.¹⁹ On average, about 96.0 wt% of Ni/C-300 catalyst can be recovered for each magnetic separation. Nevertheless, Ni particles occur to aggregate after 10 cycles to some extent, and the size is in a range of 25-70 nm, as the TEM image shown in Figure S7. The results show that the Ni/C catalysts fabricated by the strategy reported in the present study have good reproducibility, and can be used repeatedly.

Moreover, it is interesting to note that the as-made Ni/C-300 also exhibits a high catalytic performance for the selective hydrogenation of other nitroarenes to the corresponding anilines (Table 1). For the *m*-CNB and *p*-CNB, the Ni/C-300 can reach the full conversion of substrates under the general reaction conditions, as well as over 84% selectivity to *m*-CAN and *p*-CAN. Meanwhile, 100% *o*-nitrophenol, 100% *p*-nitroaniline, 65.3% *p*-nitrotoluene, and 73.1% nitrobenzene have been converted over the Ni/C-300, with *ca.* 86.4% *o*-aminophenol, 75.1% *p*-phenylenediamine, 100% *p*-methylaniline, and 96.9% aniline selectivity, respectively (Entry 4~7 of Table 1). This suggests that the Ni/C-300 is one of promising catalysts for the selective hydrogenation of various nitroarenes.

Table 1. Selective hydrogenation of various nitroarenes over the Ni/C-300.

Entry	Substrates	Products	Con (%)	Sec (%)
1			98.9	86.0
2			100	84.3
3			100	84.5
4			100	86.4
5			100	75.1



Reaction conditions: 0.50 g substrates, 0.05 g Ni/C-300, 50 mL ethanol, 140 °C, 2.0 MPa H₂, time 2 h.

Conclusions

In summary, magnetic Ni/C catalysts with a unique hierarchical structure have been prepared by directly heating sheet-like Ni(OH)₂/HTC composites at different temperatures. Among the Ni/C catalysts obtained in the present work, the Ni/C-300 has smaller Ni particles with high dispersion and unique hierarchical structure, and exhibits a much better catalytic performance for selective hydrogenation of *o*-CNB to *o*-CAN. After the reaction, the Ni/C-300 can be easily recovered by an external magnetic force, and reused for over 10 times without obvious drop in conversion of *o*-CNB and selectivity to *o*-CAN. The Ni/C-300 also exhibits a good catalytic performance in the selective hydrogenation of other various nitroarenes. The present work may provide a facile approach to synthesize the Ni/C catalysts that hold promise for the selective hydrogenation of nitroarenes to the corresponding anilines in large scale production.

Acknowledgements

This work was partly supported by the NSFC (Nos. 21336001, 21361162004), and the Education Ministry of China (No.20120041110020).

Notes and references

¹ Carbon Research Laboratory, Liaoning Key Lab for Energy Materials and Chemical Engineering, State Key Lab of Fine Chemicals, School of Chemical Engineering, Dalian University of Technology, Dalian 116024, China. E-mail: jqiu@dlut.edu.cn

² Department of Chemistry, Qingdao University, Qingdao 266071, Shandong, China.

Electronic Supplementary Information (ESI) available: Experimental results of Ni/C catalysts in selective hydrogenation of *o*-CNB; SEM images of the Ni/C-400, Ni/C-500, Ni/C-600, and Ni/C-700; TEM and magnified TEM images of the Ni/C-400 and Ni/C-700; HRTEM images of the Ni/C-400 and Ni/C-700; Nitrogen adsorption-desorption isotherms of the Ni/C-300 and Ni/C-400; Pore size distributions of the Ni/C-300 and Ni/C-400; Experimental results of the Ni/C-300 in selective hydrogenation of *o*-CNB for 10 cycles; TEM image of the Ni/C-300 after 10 cycling reactions. See DOI: 10.1039/b000000x/

- H. Blaser, H. Steiner and M. Studer, *ChemCatChem*, 2009, **1**, 210-221.
- A. Corma, P. Concepcion and P. Serna, *Angew. Chem. Int. Ed.*, 2007, **46**, 7266-7269.
- E. Gelder, D. Jackson and M. Lok, *Chem. Commun.*, 2005, 522-524.
- M. Liu, J. Zhang, J. Liu and W. W. Yu, *J. Catal.*, 2011, **278**, 1-7.
- C. J. Serpell, J. Cookson, D. Ozkaya and P. D. Beer, *Nat. Chem.*, 2011, **3**, 478-483.
- F. Wang, J. Liu and X. Xu, *Chem. Commun.*, 2008, 2040-2042.
- J. Zhang, Y. Wang, H. Ji, Y. Wei, N. Wu, B. Zuo and Q. Wang, *J. Catal.*, 2005, **229**, 114-118.
- V. Kratky, M. Kralik, M. Mecerova, M. Stolcova, L. Zalibera and M. Hronec, *Appl. Catal. A*, 2002, **235**, 225-231.
- F. Cárdenas-Lizana, D. Lamey, N. Perret, S. Gómez-Quero, L. Kiwi-Minsker and M. A. Keane, *Catal. Commun.*, 2012, **21**, 46-51.
- Y. Chen, J. Qiu, X. Wang and J. Xiu, *J. Catal.*, 2006, **242**, 227-230.
- D. He, H. Shi, Y. Wu and B.-Q. Xu, *Green Chem.*, 2007, **9**, 849-851.
- Y. Chen, C. Wang, H. Liu, J. Qiu and X. Bao, *Chem. Commun.*, 2005, 5298-5300.
- B. Zuo, Y. Wang, Q. Wang, J. Zhang, N. Wu, L. Peng, L. Gui, X. Wang, R. Wang and D. Yu, *J. Catal.*, 2004, **222**, 493-498.
- F. Cao, R. Liu, L. Zhou, S. Song, Y. Lei, W. Shi, F. Zhao and H. Zhang, *J. Mater. Chem.*, 2010, **20**, 1078-1085.
- J. Chen, N. Yao, R. Wang and J. Zhang, *Chem Eng J*, 2009, **148**, 164-172.
- X. Meng, H. Cheng, S.-I. Fujita, Y. Hao, Y. Shang, Y. Yu, S. Cai, F. Zhao and A. Masohiko, *J. Catal.*, 2010, **269**, 131-139.
- J. Xiong, J. Chen and J. Zhang, *Catal. Commun.*, 2007, **8**, 345-350.
- Y. Zheng, K. Ma, H. Wang, X. Sun, J. Jiang, C. Wang, R. Li and J. Ma, *Catal. Lett.*, 2008, **124**, 268-276.
- Y. Xie, C. Yu, N. Xiao and J. Qiu, *Catal. Commun.*, 2012, **28**, 69-72.
- N. Mahata, A. F. Cunha, J. J. M. Orfao and J. L. Figueiredo, *Catal. Commun.*, 2009, **10**, 1203-1206.
- M. Oubenali, G. Vanucci, B. Machado, M. Kacimi, M. Ziyad, J. Faria, A. Raspolli-Galetti and P. Serp, *ChemSusChem*, 2011, **4**, 950-956.
- C. Wang, J. Qiu, C. Liang, L. Xing and X. Yang, *Catal. Commun.*, 2008, **9**, 1749-1753.
- X. Xu, X. Li, H. Gu, Z. Huang and X. Yan, *Appl. Catal. A*, 2012, **429-430**, 17-23.
- C. Antonetti, M. Oubenali, A. M. Raspolli Galletti, P. Serp and G. Vanucci, *Appl. Catal. A*, 2012, **421-422**, 99-107.
- J. Wang, G. Fan and F. Li, *Catal Sci Technol*, 2013, **3**, 982.
- B. Hu, K. Wang, L. Wu, S. H. Yu, M. Antonietti and M. M. Titirici, *Adv. Mater.*, 2010, **22**, 813-828.
- M. M. Titirici and M. Antonietti, *Chem. Soc. Rev.*, 2010, **39**, 103-116.
- S. Ding, J. S. Chen and X. W. Lou, *Adv. Funct. Mater.*, 2011, **21**, 4120-4125.
- S. Ding, J. S. Chen and X. W. Lou, *Chem. Eur. J.*, 2011, **17**, 13142-13145.
- T. Zhu, J. S. Chen and X. W. Lou, *J. Phys. Chem. C*, 2011, **115**, 9814-9820.
- P. Makowski, R. D. Cakan, M. Antonietti, F. Goettmann and M. M. Titirici, *Chem. Commun.*, 2008, 999-1001.
- C. B. Putta and S. Ghosh, *Adv. Synth. Catal.*, 2011, **353**, 1889-1896.

33. L. F. Chen, H. W. Lang, Y. Lu, C. H. Cui and S. H. Yu, *Langmuir*, 2011, **27**, 8998-9004.
34. G. J. d. A. A. Soler-Illia, M. Jobbágy, A. E. Regazzoni and M. A. Blesa, *Chem. Mater.*, 1999, **11**, 3140-3146.
35. L. Xu, Y.-S. Ding, C.-H. Chen, L. Zhao, C. Rimkus, R. Joesten and S. L. Suib, *Chem. Mater.*, 2008, **20**, 308-316.
36. X. M. Sun and Y. D. Li, *Angew. Chem. Int. Ed.*, 2004, **43**, 597-601.
37. L. Yu, C. Falco, J. Weber, R. J. White, J. Y. Howe and M. M. Titirici, *Langmuir*, 2012, **28**, 12373-12383.
38. C. Falco, F. P. Caballero, F. Babonneau, C. Gervais, G. Laurent, M. M. Titirici and N. Baccile, *Langmuir*, 2011, **27**, 14460-14471.
39. L. Xing, J. Qiu, C. Liang, C. Wang and L. Mao, *J. Catal.*, 2007, **250**, 369-372.